European Journal of Pharmaceutics and Biopharmaceutics 136 (2019) 38–47

Contents lists available at ScienceDirect

European Journal of Pharmaceutics and Biopharmaceutics

journal homepage: www.elsevier.com/locate/ejpb

Research paper

Edible solid foams as porous substrates for inkjet-printable pharmaceuticals

Laura-Diana Iftimi, Magnus Edinger, Daniel Bar-Shalom, Jukka Rantanen, Natalja Genina*

University of Copenhagen, Department of Pharmacy, Universitetsparken 2, DK-2100 Copenhagen, Denmark

ARTICLE INFO

Keywords:
Solid foam
Freeze-drying
Substrate
Inkjet printing
Mechanical properties

ABSTRACT

The aim of this study was to investigate new porous flexible substrates, i.e., solid foams that would serve as a carrier with a high ink absorption potential for inkjet printable pharmaceuticals. Propranolol hydrochloride was used as a model active pharmaceutical ingredient (API). Pharmaceutically approved and edible cellulose derivatives and gums together with different additives were evaluated as a base for the substrate. Different methods for preparation of a solid foam such as freeze-drying, vacuum oven drying and drying at room temperature were explored. Only freeze-drying of the polymeric solutions resulted in the desired porous and flexible, but mechanically stable, soft sponge-like substrates with hydroxypropyl methylcellulose (HPMC)-based solid foams being the most suitable for the use in continuous inkjet printing. The plasticized HPMC foams had a superior absorption capacity and fast penetration speed for the different solvents due to the open cell pore structure and higher porosity as compared to nonplasticized additive-free foams, although, the latter were less hygroscopic. The produced solid foams were well suited for inkjet printing of high volumes of API-containing ink. The inkjet-printed API was immediately released from the dosage forms upon contact with the dissolution medium. This work demonstrates that the fabricated solid foams, based on plasticized HPMC, show a great potential as porous carriers in the fabrication of high dose dosage forms by inkjet printing.

1. Introduction

Personalized medicine, often referred in the scientific literature as precision, individualized or stratified medicine, is a recent strategy towards improvement of healthcare, where the main focus is narrowed down to individual level rather than to the average response of a group with potential cost savings and enhanced therapeutic efficiency [1–3]. Currently, the availability of a medicine in only two or three different strengths limits the possibility of a tailored per needs treatment. The industrial scale production ignores 'different than the rest' medical needs and therefore, innovative manufacturing methods are desired, satisfying the following criteria: (*i*) flexibility in titration of the required dose, (*ii*) precise dosing of active pharmaceutical ingredient (API), (*iii*) high-throughput capacity and ideally, (*iv*) the possibility of preparing medicines at the point-of-care [4,5].

Pharmacoprinting – inkjet printing of APIs, as a part of additive manufacturing technique, is a new method in pharmaceutical technology, and it has been reported to nearly cover all the aforementioned issues [6,7]. Pharmacoprinting by inkjet printing is based on the precise transfer of an API-containing ink onto a carrier substrate in a computer-controlled way. A variety of APIs, including problematic drugs, such as poorly soluble APIs or proteins, have been formulated as solutions or (nano)suspensions and successfully dispersed onto suitable carrier substrates, obtaining solid dosage forms suitable for oral administration [8,9]. Placebo tablets [10,11], orodispersible films [12] and oral non-porous films/sheets [13–15] have been used as edible carrier substrates for printable pharmaceuticals. The printing resolution, the concentration of the drug in the ink, the size of printed area on the substrate and the number of printed layers can be easily modified in order to obtain a defined amount of API in the dosage unit [13,14,16].

However, earlier studies have concluded that 2D printing is better suited for low dose, highly potent APIs and paediatric formulations, because the main limiting factor is the low ink absorption capacity of the mainly non-porous substrates used, limiting the amount of ink that it is possible to incorporate per unit area without affecting the integrity and mechanical properties of the substrate [6]. An increase in the area printed and concentration of the drug in the ink can address this obstacles, but the former is limited to the practically administrable dimensions of the substrate [17] and the latter is constrained by the solubility of the drug in the ink. Highly concentrated nanosuspensions have been used with limited success [18].

Alomari et al. [6] pointed out that future research should be focused on the development of pharmaceutically approved substrates that promptly absorb the ink. Recently, porous substrates with an increased

* Corresponding author.
E-mail address: natalja.genina@sund.ku.dk (N. Genina).

https://doi.org/10.1016/j.ejpb.2019.01.004
Received 25 June 2018; Received in revised form 15 December 2018; Accepted 6 January 2019
Available online 08 January 2019
0939-6411/

area to volume ratio were proposed for manufacturing of printable pharmaceuticals [11,19–21]. For instance, Palo et al. [20] printed lidocain-containing ink on gelatine-based electrospun highly porous fibrous matrix, containing piroxicam. It is well-known that electrospinning offers very little control over pore size distribution and fibrous alignment [22–24]. In addition, obtaining a stress-resistant electrospun matrix can be challenging. Edinger et al. [11] developed a hydroxypropyl methylcellulose (HPMC)-based solid and flexible foam, using vacuum oven drying. However, the resulting foam had a closed-cell structure with a continuous film on its surface that restricted penetration of API-containing ink into the foam. Small-sized porous thin substrates, containing only HPMC, were prepared by freeze-drying to be covered with nonporous HPMC film after API-deposition by an electrodeless electrohydrodynamic method for fabrication of personalized dosage forms [21]. However, manufacturing procedure, optimization and characterization of the properties of the substrates were not considered in that study.

In the present study, solid mechanically stable foams were developed by drying different polymeric solutions in a vacuum oven and a freeze-dryer. The freeze-drying method yielded uniform, open-cell porous structures as compared to the vacuum oven. Pharmaceutical lyophilizates, also called wafers, as new carrier systems possess high porosity (30–50%), consisting of interconnected channel with open-cell structure, and fast rehydration tendency [25]. These favourable characteristics make the freeze-dried wafers promising candidates for printable pharmaceuticals [21]. Frequently, an API is added into polymeric gel to obtain the final dosage forms after freeze-drying. However, incorporation of the drug within the gel before the drying step could inevitably affect the chemical and physical stability of the API during the process and on storage. Therefore, manufacturing of placebo porous substrates in advance and printing API-containing ink on-demand could avoid this problem.

The current study was focused on the development of the new porous highly flexible, but at the same time mechanically stable substrates that would be suitable for the printing of high volumes of the API-containing ink. Different polymeric and gummy solutions with plasticizers and other additives were freeze-dried, vacuum oven dried or dried at room temperature (RT). The three most suitable candidates, based on hydroxypropyl methylcellulose (HMPC), were screened out and then characterized among others for microscopic structure, using scanning electron microscope; porosity with oil absorption method, mechanical properties by texture analyser in tensile strength and compression mode; drop absorption speed by drop shape analyser and hygroscopicity by using dynamic vapour sorption. These substrates were used to produce inkjet-printed propranolol-containing dosage forms, and their suitability for inkjet printing of high dose dosage forms was evaluated. Release studies were carried out in simulated saliva buffer solution, revealing a potential usage of the developed dosage forms also for oromucosal delivery.

2. Materials and methods

2.1. Materials

The following excipients were used as a main component for substrate preparation: hydroxypropyl methylcellulose (HPMC), Metholose® 60SH-50 and Metholose® 60SH-4000 with 50 and 4000 mPa s labelled viscosity, respectively, and methylcellulose (MC), Metholose® 60SM-4000 from Shin-Etsu Chemical, Tokyo, Japan; hydroxypropyl cellulose (HPC), Klucel® LF (Aqualon™, Ashland, Netherlands, with 50 mPa s labelled viscosity), xanthan (Sigma-Aldrich, USA), agar (Sigma-Aldrich, Spain), guar gum (Sigma-Aldrich, Pakistan). Various additives were added to the base of the substrate to change its properties: poloxamer 188, Lutrol® F68 (Sigma-Aldrich, Steinheim, Germany), polyethylene glycol 4000, PEG4000 (Fluka Analytical, Germany), glycerol (Sigma-Aldrich, Germany), polysorbate 20, Tween® 20 (Fluka Analytical, Switzerland) and sodium lauryl sulphate, SLS (Unikem, Copenhagen, Denmark). Propranolol hydrochloride as a model drug was purchased from Sigma-Aldrich (Germany). E133 brilliant blue (Dr. Oetker, Helsinki, Finland) was used as a coloring agent. Polylactic acid (PLA) 2.85 mm filaments (Innofil3D®, Emmen, Netherlands) were used for obtaining customized water insoluble in-house 3D printed molds for mechanical analysis. The chemicals and solvents were of analytical grade and used without further purification.

2.2. Methods

2.2.1. Substrate preparation

The polymer/gums with and without the different additives of the matrix were accurately weighed and triturated in a mortar with a pestle (only if additives were used). The powder blend was gradually poured into 100 ml of preheated up to 70–80 °C distilled water under a vigorous stirring, using a magnetic stirrer (IKA® RH Digital, Germany) until a uniform viscous solution was formed. Both grades of HPMC were used at concentration 2.5 and 5.0 (w/v%), whereas MC, HPC and agar were used only at 5.0 (w/v%). The mixture of xanthan:guar (1:1) at 3.0 (w/v%) was used [26]. The additives were incorporated at the three levels: 10, 20 and 30% w/w of polymer/gum solid content for PEG 4000, Tween® 20 or glycerol, and 3.3, 16.7 and 33.3% of polymer/gum solid content for SLS and Lutrol F® 68. Each polymer at each concentration was tested with each level of a single additive and all combinations of two, three and four additives at concentration of 10% w/w of polymer/gum solid content for PEG 4000, Tween® 20 or glycerol, with and without 3.33% w/w of polymer/gum solid content for SLS and Lutrol F® 68. In total, 200 different formulations were prepared to be used for substrate preparation at RT, in vacuum oven and freeze-drier (Supplementary data 1).

The obtained polymer/gum solutions were poured into commercially available silicon bread molds (FUNKTION, Viborg, Denmark) and kept overnight in the fridge (2–8 °C) to allow a complete hydration of the polymer/gum and degasing of the poured liquid. The solutions, covering an area of 280 × 65 mm^2 with a thickness of 5 mm were freeze-dried using an Epsilon 1–4 LSCplus laboratory scale freeze-dryer (Martin Christ, Germany). The freeze-drying cycle consisted of freezing to – 30 °C in 3 h and holding at – 30 °C for 3 h. Then the pressure was reduced and kept constant at 0.12 mbar during subsequent primary drying at 0 °C for 16.5 h. This shelf temperature (0 °C) was reached in 50 min.

The vacuum drying was performed according to the previously described by Edinger et al. method [11]. All the obtained polymer/gum solutions were foamed with a hand blender, casted with a spatula in Petri dish and placed in the vacuum oven at 60 °C and 40 mbar for 24 h. The other casted Petri dishes were left to dry at room temperature for 24 h.

After drying the samples were stored in the tightly closed plastic bags at room temperature until further analysis.

2.2.2. Microscopic analysis

Samples were carefully cut using a scalpel and coated with gold for 15 s with sputter coater 108auto (Cressington Scientific Instruments, Watford, UK) and scanned with a TM3030 Tabletop scanning electron microscope (SEM) (Hitachi Power Tools Denmark A/S, Esbjerg, Denmark) at 5 kV and 100–500× magnification.

2.2.3. Drop penetration speed

The measurement of the speed of the drop sorption onto the prepared substrates was performed with a Drop Shape Analyzer DSA100 (KRÜSS, Germany). Distilled water, ethanol and silicon oil were used as the solvents. A sessile drop of approx. 30 µl was generated by a manually acted syringe (diameter of the needle = 1.83 mm). A single droplet was applied and the speed of the drop penetration was measured using the built-in video camera. The time point when the droplet

was not visible anymore was determined. The measurements were performed at room temperature and the sample size of the substrate was chosen similar to the printed dosage form (1 × 1 cm^2).

2.2.4. Vapour sorption and desorption analysis

Dynamic vapour sorption and desorption analysis was undertaken with the use of VTI-SA + analyser (TA Instruments, New Jersey, USA). The gravimetrical response of the blank substrates upon the relative humidity (RH) change from < 5% to 95% RH and back to < 5% in steps of 10% (5% for 95% RH) was recorded. Approximately 10 mg of the blank substrate was placed in a glass pan. The cycle started by drying the sample at 60 °C for up to 3 h with a temperature increment of 2 °C. Afterwards, the temperature was kept at 25 °C for the entire measurement.

The samples were stored in desiccators at < 5%, 23%, 43%, 75% and 95% RH over 3 months at 22 ± 1 °C. The required RH was achieved using fumed silica and saturated solutions of potassium acetate, potassium carbonate, sodium chloride and potassium nitrate, respectively.

2.2.5. Swelling analysis

Accurately weighted samples in the range of 37 ± 8 mg were placed in 100 ml of water. The change in the mass was recorded at 2, 5, 10, 20 and 30 min, and the gain in the mass was calculated according to Eq. (1), where M_o and M_t are the mass of the foams before contact with water and after swelling at time t, respectively:

$$Swelling\ \ index\ \ (\%) = \frac{Mt - Mo}{Mo} * 100\% \quad (1)$$

2.2.6. Porosity analysis

The porosity of the substrates was measured using a slightly modified oil absorption technique described previously for measuring the porosity of roller-compacted ribbons [27]. Samples of approx. 12 mm by 12 mm were cut out carefully using a scalpel and the samples were weighed and the dimensions were measured using a caliper. The samples were placed in paraffin oil in a desiccator with fumed silica and subjected to a vacuum for 24 h. After this the samples were taken out of the oil and excess oil was carefully wiped off using a Kleenex® tissue. The samples were then weighed and the absorption capacity was determined as the amount of oil absorbed divided by the mass of the untreated samples. Films made from the same polymeric solutions as the foams were prepared and dried at room temperature. The oil absorption capacity of the films was then compared in a similar manner.

2.2.7. Texture analysis

TA XT.Plus (Stable Micro Systems, Godalming, UK), equipped with a load cell with a maximum load of 50 N and a resolution of 1 N, was used for recording the mechanical properties of the blank solid foams. The samples for the mechanical analysis were prepared by freeze-drying the polymer solutions as mentioned above in the customized molds that were designed using an online computer-aided design program (Tinkercad, 2017) and in-house 3D printed with a MakerBot Replicator Desktop 3D printer (Brooklyn, USA) (Supplementary material 2). This was done in order to get samples of the same size without the need of punching out the required shape from a bigger piece of the foam, and hence avoid the effect of the applied stress on the subsequent results. Two operational modes were selected: tensile strength and compression. For the former mode, the rectangular wafers (2 by 7 cm^2) were fixed between the tensile grips and the change in length (% strain) of the sample was recorded against the applied stress (N/mm^2) at a test speed of 5 mm/s and a trigger force of 0.049 N with a gripping distance of 20 mm. For the latter mode, cylindrical wafers (diameter = 2 cm, height = 1 cm) were placed on the support and a 6 mm diameter stainless steel cylindrical probe was set to deform the sample to a depth of 3 mm with a trigger force of 0.049 N at a test and post-test speed of 2 mm/s. Before measurements, the dimensions of the foams were measured in different areas using a digital caliper (Mitutoyo Corporation, Kawasaki, Japan).

2.2.8. Ink formulation

The well-printable ink was prepared by using a slightly modified formulation as presented by Genina et al. [28]. Namely, a solution of 50 mg/ml propranolol in 30:70 propylene glycol:water (vol%) was prepared and 0.4% (vol%) of colorant E133 brilliant blue was added for visualization purposes.

2.2.9. Inkjet printing

The printing of the dosage forms on the developed substrates was performed with a PiXDRO LP50 piezoelectric inkjet printer (Roth & Rau, Eindhoven, Netherlands) equipped with a Spectra SL-128 AA print head and 128 jetting nozzles (Fujifilm, Tokyo, Japan), each with a diameter of 50 µm. Prior to printing, the ink was filtered using a 0.45 µm polypropylene membrane filter (VWR International, USA). Separately, a printing pattern of 1 cm × 1 cm (177 pixel × 177 pixel) was designed in Microsoft Paint v. 1607 software, obtaining an image of 42 squares with 5 mm spacing between the squares. The amount of squares was reduced during printing of multiple passes to produce the dosage forms, containing different doses. The printing was performed at the head voltage of 92 V, the pulse shape 3–14-5 µs, the ink pressure of −21.3 mbar (negative pressure was needed to prevent leaking of the ink from the nozzle), the frequency of 925 Hz and the resolution of 450 dpi. The developed substrates were placed directly on the vacuum clamped polyethylene terephtalate sheets at – 50 mbar (negative pressure was needed to ensure a proper attachment of the sheets to the substrate's holding plate). The printing was performed in ambient conditions.

2.2.10. Thermal analysis

Thermogravimetric analysis (TGA) was performed by placing the blank substrates in platinum pans (100 µl) and heating them from 25 °C to 250 °C at a heating rate of 5 °C/min, using Discovery TGA (TA Instruments, New Castle, USA). The measurements were performed in triplicate and the values for weight loss (%) at 110 °C were presented as mean value ± standard deviation.

Differential scanning calorimetry (DSC) of the printed and unprinted samples was done by accurately weighing the samples of 1–4 mg and placing in aluminium pans with lids. The samples were run on a Discovery DSC (TA Instruments, New Castle, USA) and scanned from −80 °C to 200 °C at 10 °C/min. Modulated differential scanning calorimetry (MDSC) analysis was conducted on the samples with 15–20 mg used for the blank substrates and 7–10 mg used for propranolol powder. They were scanned from 50 °C to 200 °C at a heating rate of 1 °C/min with a modulated amplitude and period of 0.8 °C and 60 s, respectively.

2.2.11. High performance liquid chromatography (HPLC)

In order to determine the amount and release profile of propranolol from the printed samples, a HPLC instrument Agilent 1290 Infinity® (Agilent Technologies, Germany), equipped with a Luna® 5 µm C18(2) 100 Å 150 × 4.6 mm LC column (Phenomenex, Denmark) was used, applying slightly modified parameters as described by Modamio et al. [29]. The mobile phase was composed of 60:40 (vol%) 0.067 M phosphate buffer (pH 3):acetonitrile used isocratically at a flow rate of 0.8 ml/min. The injection volume was 10 µl and the wavelength for the API detection was set at 294 nm. Linearity was observed between 1 and 500 µg/ml (R^2 = 0.9999).

2.2.12. Drug content

Drug content was determined by cutting out the printed dosage forms, containing low, medium and high printed doses, and immersing each of them into 50 ml of freshly prepared simulated saliva buffer at

37 °C, according to Palo et al. [20], and stirring them for 3 h. The prepared solutions were centrifuged at 2000 rpm for 1 min and the obtained supernatant was analysed by HPLC.

2.2.13. Release studies

The release studies were performed using simulated saliva buffer. The printed dosage forms of low, medium and high doses (n = 3) were placed into 50 ml of the freshly prepared saliva buffer at 37 °C and stirring rate of 200 rmp, using a hotplate stirrer with the thermoregulator (IKA® RH Digital, Germany). Samples of 1 ml were collected at predetermined time intervals of 0, 1, 2, 5, 10, 15, 30, 60, 120 and 180 min and replaced with preheated pure saliva buffer. The collected samples were processed and analysed as described the previous section. The release studies were conducted under sink conditions.

3. Results and discussion

3.1. Fabrication and visual observation of the substrates

The ideal substrate for inkjet printing of the API-containing ink would be a uniform, edible and flexible porous open-cell carrier that could be produced in large sheets to allow continuous roll-to-roll printing as described by Borges et al. [30]. Furthermore, it should have a high ink absorption capacity to allow fabrication of both low and high dose dosage units [6]. This means that the substrate should be relatively thick as opposed to oral strips [30] and that the printing surface should present open pores without a nonporous polymeric film, at least on the printable surface, to allow a high volume of the ink to be efficiently incorporated in the carrier without the ink going through and leaking from the substrate. Furthermore, the ideal substrate should remain intact after deposition of high volume of the ink followed by a possible drying step [14]. This means that extensive disintegrations and/or dissolution of the substrate in contact with the ink should not take place. The ideal carrier should be non-hygroscopic to withstand any fluctuations in the ambient conditions and microbiological contamination and, thereby, minimize the cost spent on the packaging of the final dosage forms. For instance, one of the reasons for the small number of drug-containing oral films available on the market is costly packaging [31]. Last, easy cuttability with a blade and non-sticky nature of the substrate would allow manufacturing multiple doses on the same carrier and afterward dividing the desired dose.

Encouraged by the fact that paper-like [12] and/or wafer/sponge-like carriers [32,33] showed promise for pharmacoprinting, other pharmaceutically approved edible excipients and preparation methods that could yield substrates with the desired properties were considered. There is a bewildering number of polysaccharides with different properties, molecular weights and substitution levels which potentially could be useful. Gum-base substrates such as agar, xanthan and guar, and cellulose derivatives such as HPMC, HPC and MC with and without plasticizers and other additives were screened for suitability as potential candidates. Agar was selected based on the outcomes of a previous study [34]. Xanthan-guar porous matrices were previously obtained as nasal inserts [26]. The porous structure of freeze-dried HPMC hydrogels was intensively described in the literature [35]. HPC and MC were chosen due to structural similarity with HPMC. In the present work, an attempt was made to select polymers from different origins and different qualities hoping that in the future it will be possible discern a pattern enabling a more systematic selection. Based on the scientific literature, freeze-drying [21,33,36,37] was chosen as a potential technique for preparation of porous substrates for inkjet-printable pharmaceuticals, whereas drying in vacuum oven [11] and drying at room temperature (RT) were used as comparison methods. As expected, porous albeit thin films of different flexibility from gummy excipients were obtained after vacuum drying and drying at RT, whereas only the freeze-drying method led to formation of solid porous foams. Agar-based forms were brittle and fragile even after the addition of a plasticizer up to 30% (w/w), whereas xanthan-guar wafers were very hard to cut and they appeared dusty upon cutting (Supplementary material 3). Therefore, further work with gum-based foams was discontinued.

Cellulose-derivatives dried at RT yielded nonporous thin films of satisfactory flexibility with addition of plasticizers and other additives. This is in accordance with the literature when solvent casting of cellulose-solutions with a high and uncontrolled water evaporation rate was used for preparation of oral nonporous films [17]. After a vacuum drying the polymeric solutions transformed into solid foams with uneven pore size distribution, especially, when SLS was present. However, all the open-cell structures had a visible nonporous film on their surface, sealing the pores (Supplementary material 4). The formation of the superficial continuous 'skin' layer can be explained by a high concentration of the polymer on the top of the porous structure due to a gradual rather than homogeneous and simultaneous drying [38]. Only the freeze-drying method led to visually homogeneous solid foams without any visible sign of continuous film formation on the surface. The formed sponge-like structures preserved the "volume" of the initial height of the viscous solution and the shape of the casting mold. The obtained freeze-dried foams were self-preserved, compared to the solid matrix prepared at RT and vacuum oven, where signs of microbiological contaminations were noticed upon one month storage in the ambient conditions. This can be related to the higher water activity of the fabricated films as compared to the foams however, this finding needs further investigation.

Different matrix-forming polymers and additives at different concentrations resulted in solid foams of different properties. The foams with a high amount of plasticizers were not completely dried. Plasticized and unplasticized HPC foams had a rigid structure that was difficult to cut, whereas MC foams were electrostatically charged even when additives were included. Mechanical flexibility of the HPMC-based foams decreased with an increase in the content and viscosity grade of the polymer. It was noticed that the presence of SLS in the formulation yielded foams with less uniform pore size distribution. Based on the visual observation of the morphological appearance, porosity, pore size distribution, flexibility, microbiological stability and cuttability of the freeze-dried foams, three substrates based on HPMC (Metolose® 60SH-4000) were chosen for further analysis and inkjet printing of API-containing inks at the top side of the substrate with subsequent characterization of the obtained dosage forms (Table 1).

Table 1
The composition of the selected substrates, based on hydroxypropyl methylcellulose (HPMC) (Metolose® 60SH-4000).

	Polymer		Additives	
Substrate	Name	[ ] (w/v%) in water	Name (ratio)	%w/w of polymer solid content
S1	HPMC	5	–	–
S2	–″–	–″–	PEG 4000: Tween® 20:Glycerol (1:1:1)	30
S3	–″–	–″–	PEG 4000: Tween® 20:Glycerol (1:1:1) + Lutrol® F68	30 + 3.3

PEG 4000 = polyethylene glycol 4000; Tween® 20 = polysorbate 20; Lutrol F® 68 = poloxamer 188.

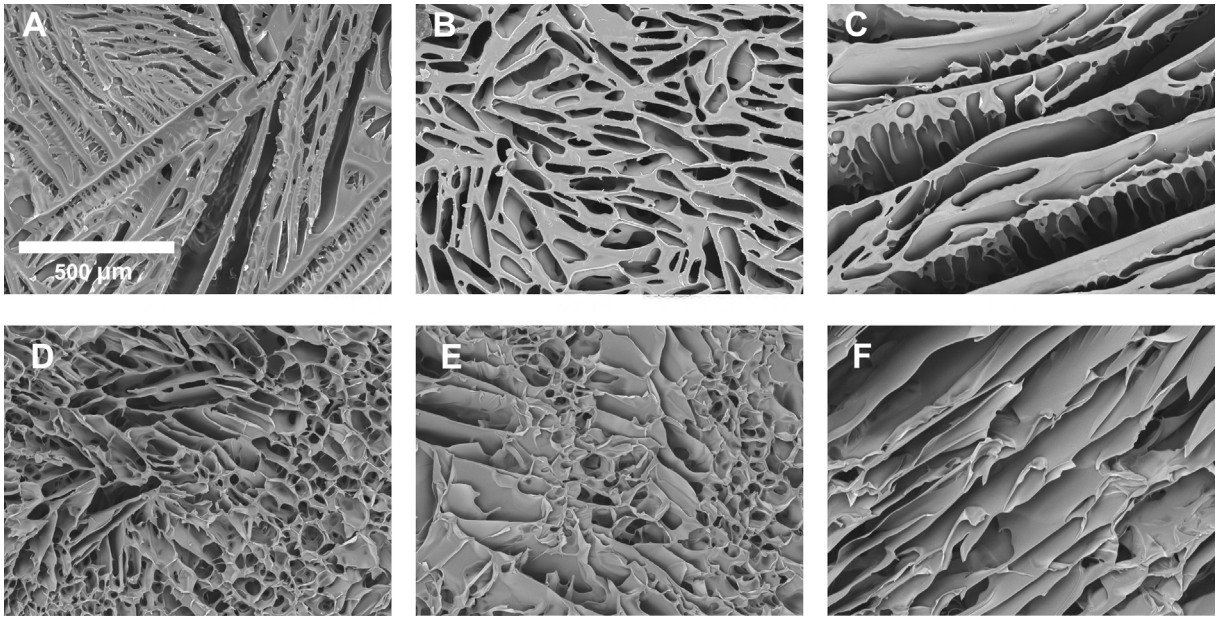

Fig. 1. Scanning electron micrographs of the surface (top) and cross-section (bottom) of substrates S1 (A, D), S2 (B, E) and S3 (C, F).

3.2. Characterization of the substrates before printing

3.2.1. Microscopic observation

A thorough morphological analysis, using SEM, confirmed that all blank substrates possessed open pore structures without any non-porous 'skin' layer on their surface (top side of the substrate) (Fig. 1). However, the obtained substrates possess different surface topography. Substrates **S1** and **S3** had a surface pore structure with needle-shaped pattern, indicating that large ice crystals were formed during freeze drying. The surface of substrate **S2** consisted of relatively small homogeneously sized pores. The internal structure of the samples revealed some variation in the sizes of the pores. Substrate **S1** and **S2** exhibited small round pores, interspersed with needle-shaped pores. In turn, **S3** had mostly oblong needle-shaped pores. An ideal substrate should have large pores with even pore size distribution on both the surface and inside the substrate to allow incorporation higher volumes of ink and to avoid variation in the absorption capacity of the substrates during printing. The obtained results make substrate **S3** the most favorable in this regard. It is worth mentioning that all substrates possessed the less porous surface at the bottom side (towards the mold) than the surface at the top side (data not shown).

The porosity measurements of the samples showed that the substrate **S1** was the least porous, while **S3** was the most porous (Table 2). At the same time the substrate with the lowest oil absorption capacity had the highest density and vice versa. This is expected since a higher density means a less porous structure within the samples. The obtained freeze-dried substrates **S1**, **S2** and **S3** had at least 27-fold higher absorption capacity than the corresponding oral films dried at RT, highlighting their superior properties for fabrication of inkjet-printable pharmaceuticals (Table 2).

It is worth mentioning that in the present work the freeze-drying cycle was designed to yield solid porous foams from the studied polymer solutions. In the future thorough optimization of the process parameters for each formulation should be done to modulate the pore size and size distribution of the substrates, for instance, by including the annealing step above T_g' of the polymer solution to increase porosity of the substrates by affecting the size of ice crystals [39,40] and/or by modulating the freezing rate to yield the desired porosity of the substrate. However, this was outside the scope of the current study.

3.2.2. Absorption speed, swelling, moisture content and hygroscopicity of the substrates

To study the wetting properties of the selected substrates in contact with the ink of different composition and, by that, reveal the absorption and penetration ability of the substrates towards the ink during inkjet printing, measurements of absorption speed of the drop of different solvents (water, ethanol and silicon oil) were performed. The results for water showed that the substrates **S2** and **S3** had a superior affinity towards water, where the drop of the solvent disappeared within 20 s when brought in contact with the substrate (Table 2). This can be attributed to the presence of the hydrophilic additives in the composition of **S2** and **S3** as compared to **S1**. In case of ethanol and silicon oil, fast wetting dynamics of less than 0.5 s were observed for all substrates (data not shown). In general, the substrate with fast ink wetting properties would be considered as the first choice due to its rapid ink absorption ability. Therefore, the substrates **S2** and **S3** would definitely suit with water, ethanol or oil-based inks.

The swelling index of the fabricated foams was 727% ± 45% for **S1**, 879% ± 63% for **S2** and 1073 ± 76% for **S3**, after 30 min of aqueous hydration. The swelling properties of the substrates **S2** and **S3** were significantly different from **S1** and from each other ($p < 0.05$). Substrates **S2** and **S3** hydrated much faster than **S1**, being fully

Table 2
Density, oil absorption capacity and water drop penetration speed of freeze-dried samples S1, S2 and S3 as well as oil absorption capacity of the solvent-casted films. Values are present as mean ± standard deviation (n = 3).

Substrate	Density (g/cm^3)	Oil absorption capacity (w/w%)	Oil absorption capacity of films (w/w%)	Water penetration speed (s)
S1	0.099 ± 0.002	786 ± 11	25 ± 14	821.2 ± 58.3
S2	0.095 ± 0.002	835 ± 15*	31 ± 16	21.2 ± 4.7*
S3	0.082 ± 0.004*	960 ± 9*	36 ± 12	18.7 ± 5.3*

* $p < 0.05$, significant difference compared to the substrate S1 by Student's unpaired *t* test.

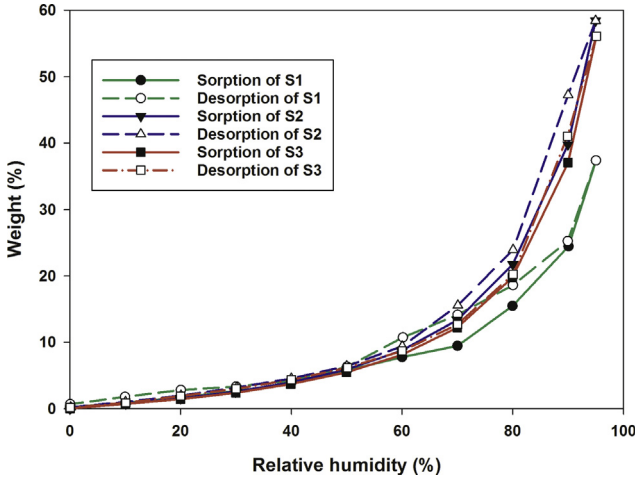

Fig. 2. Sorption/desorption profiles for the substrates **S1**, **S2** and **S3**.

hydrated after 5 min, while it took 30 min for **S1** to fully hydrate. This is also likely due to the addition of hydrophilic additives to **S2** and **S3**. Furthermore, the higher swelling index of **S2** and **S3** can also be explained by the superior porosity of those substrates as compared to **S1** (Table 2).

The thermogravimetric analysis revealed that moisture content of the substrates **S1**, **S2** and **S3** were 0.99 ± 0.12%, 1.78 ± 0.14% and 2.40 ± 0.20%, which is within the typical range of 0.5–3% for lyophilized products [40]. The determined water sorption/desorption profile of the substrate **S1** (Fig. 2) was very similar to the one of HPMC powder reported in the literature [41]. The significant weight gain of the **S1** was observed after 70% relative humidity (RH), reaching 38% equilibrium moisture at 95% RH. The sorption/desorption profiles of the substrates **S2** and **S3** were very close to each other with **S2** being slightly more hygroscopic. This small difference can be explained with the presence of poloxamer 188 that is known to be hygroscopic only at RH higher than 80% [42]. The maximum detected weight gain was 60% for both **S2** and **S3**. This leads to the conclusion that the substrate **S1** was the least sensitive to the changes in the RH. This substrate would be the most desired if the printing and subsequent storage of the dosage forms would be performed at RH higher than 60%.

It is worth noticing that the appearance of the substrates after storage at < 5%, 23%, 43%, 75% and 95% RH over three months did not change. The formation of gels out of the solid foams was not detected even at 95% RH, highlighting the ability of the developed foams to maintain the structure in harsh storage conditions.

Table 3
Young's modulus, ultimate tensile strength (UTS) and elongation at break values for the studied substrates S1, S2 and S3. Values are presented as mean ± standard deviation, n = 3.

Substrate	Young's modulus (mN/mm^2)	Ultimate tensile strength (mN/mm^2)	Elongation at break (%)
S1	35.1 ± 2.7	208.0 ± 55.4	9.4 ± 1.9
S2	12.2 ± 1.8*	82.4 ± 28.1*	23.5 ± 3.1*
S3	19.7 ± 3.4*	218.9 ± 81.5	20.6 ± 5.3*

* $p < 0.05$, significant difference compared to the substrate S1 by Student's unpaired *t* test.

3.2.3. Mechanical properties

Texture analysis of the selected substrates was undertaken to investigate their flexibility, strength and hardness. The measured stress-strain curves of the studied samples revealed rather a ductile than brittle behavior of the substrates with three distinct regions: the elastic region, the plastic region and the failure region (Fig. 3A).

In order to compare the flexibility of the different substrates, the Young's modulus or elastic modulus was determined by calculating the slope of the stress-strain curve in the elastic region. A stiffer material yields a higher value of the slope. As expected, addition of plasticizers improved the flexibility of the substrates with sample **S2** being the most flexible (Table 3). This can be explained with the increased mobility of the polymer chains in samples **S2** and **S3** due to the increased free volume between the polymer chains as a result of the incorporated plasticizers and higher detected moisture content [43]. However, the substrate **S2** appeared to be the least resistant to the applied force as its ultimate tensile strength (UTS, represents the maximum stress that a material can withstand before breaking) was lowest. Interestingly, the substrate **S3** had the highest value of UTS in spite of its relatively low elastic modulus. To evaluate the maximum deformation of the materials at the applied stress, the elongation at break (the maximum strain at which the breakage occurs) was determined. The substrate **S1** had the lowest elongation at break, whereas **S2** had the highest. These findings make the substrate **S3** the most suitable candidate from the point of view of the mechanical properties as it is flexible, and can withstand the stress and deform without an immediate breakage, when, for instance, roll-to-roll manufacturing would be required. In addition, adequate flexibility of the substrate would be beneficial, when folding of it would be needed, for instance, for loading of the produced dosage form into a hard capsule.

To evaluate the mechanical properties of the solid foams upon compression 'hardness', relaxation distance, compaction index and recovery ratio were determined (Fig. 3B) (Table 4). Peak force or

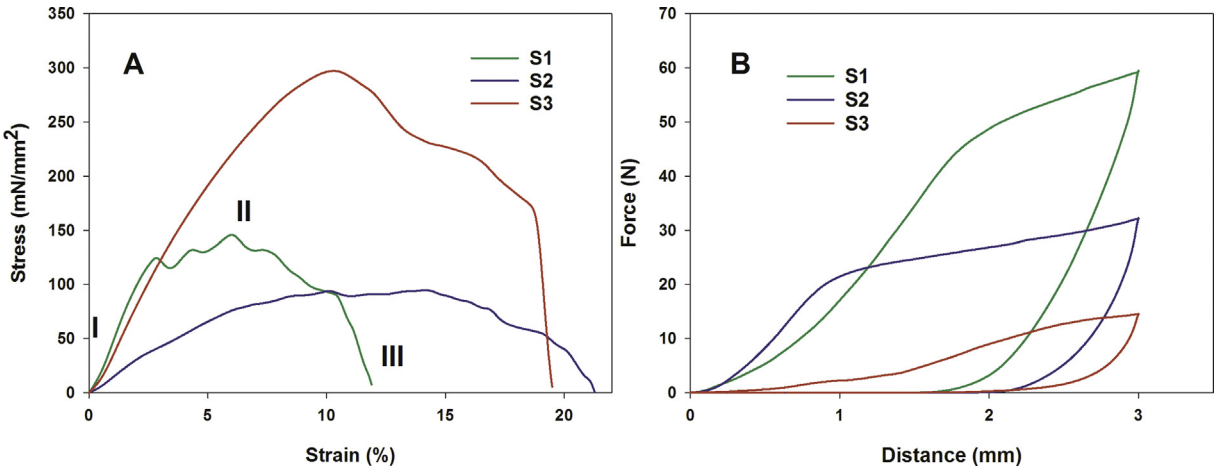

Fig. 3. (A) Representative stress-strain profiles of the substrates **S1**, **S2** and **S3**. Three distinct regions are pointed out for S1: elastic (I) plastic (II) and failure (III); (B) Representative compression profiles of the substrates **S1**, **S2** and **S3**.

Table 4
Mechanical properties of the substrates **S1**, **S2** and **S3** upon compression. Data are present as mean ± standard deviation, n = 3.

Substrate	Peak Force (N)	Relaxation distance (mm)	Compaction index (mm)	Recovery ratio (%)	Work of compression (N/mm)
S1	60.2 ± 4.1	2.4 ± 0.0	0.7 ± 0.0	27.5 ± 1.2	96.9 ± 10.0
S2	40.5 ± 8.3*	2.3 ± 0.1*	0.8 ± 0.1*	33.2 ± 2.7*	73.4 ± 10.9
S3	11.3 ± 2.8*	2.0 ± 0.2*	1.0 ± 0.1*	53.3 ± 13.7*	14.7 ± 3.1

* $p < 0.05$, significant difference compared to the substrate S1 by Student's unpaired *t* test.

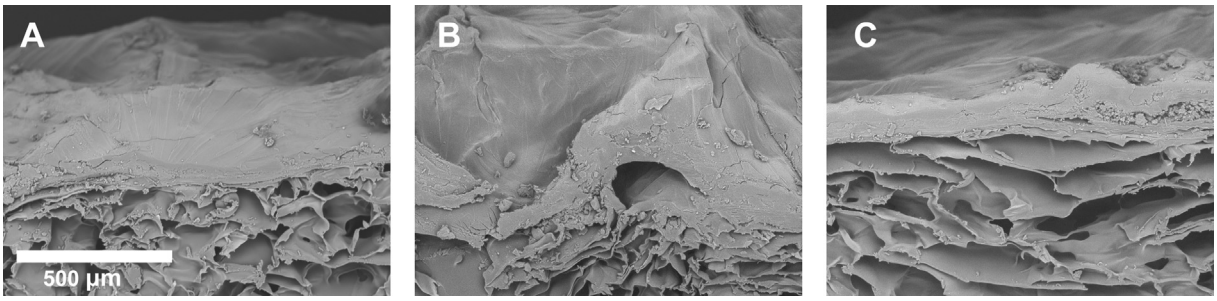

Fig. 4. Scanning electron microscopy images of a cross section, containing the drug-printed surface and the porous structure beneath the surface for substrate S1 (A), S2 (B) and S3 (C) The substrates were inkjet-printed with 20 passes.

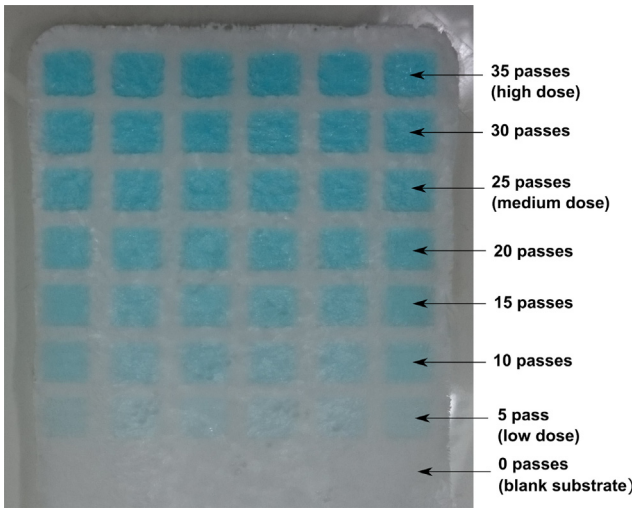

Fig. 5. The photograph of API-printed substrate **S3**, containing seven different doses. One square is equal to 1 cm^2.

Table 5
Drug content in the printed dosage forms of low, medium and high doses of substrates S1, S2 and S3. Data are presented as mean ± standard deviation, n = 3.

No. passes	Drug content, mg (mg/pass)		
	S1	S2	S3
5	0.52 ± 0.01 (0.10)	0.66 ± 0.04 (0.13)*	0.66 ± 0.01 (0.13)*
25	3.31 ± 0.03 (0.13)	3.34 ± 0.14 (0.13)	3.34 ± 0.04 (0.13)
35	4.39 ± 0.12 (0.13)	4.59 ± 0.11 (0.13)	4.68 ± 0.06 (0.13)*

* $p < 0.05$, significant difference compared to the substrate S1 by Student's unpaired *t* test.

'hardness represents the resistance of the material to compressive deformation [32]. Incorporation of the additives in the composition of the foams decreased 'hardness' of the substrates as the substrate **S1** showed the highest resistance to compression, whereas the lowest peak force was detected for **S3**. This correlates well with the porosity measurements, where **S3** appeared to be the most porous and the least dense, while **S1** was the least porous and the densest. It is also in accordance with the literature, where the plasticized wafers were weaker and less brittle compared to unplasticized ones [40]. Relaxation distance represents the difference between corresponding distance at peak force (3 mm) and the point at which the force returns to zero. The foams **S1** and **S2** showed a similar relaxation distance, whereas this parameter was significantly lower for **S3**. The compaction index is the difference in distance between the points at peak force (3 mm) and relaxation [32]. It indicates how much of the sample height could be reduced by compression. The order of the substrates, concerning the values of the compaction index, was opposite to the order of the substrates according to relaxation distance. Recovery ratio represents the ratio between the compaction index and relaxation index. It shows how well the sample is able to regain its original shape. It was found that the substrates were able to recover their initial shape upon the release of the force with 28%, 33% and 53% regain of the initial height for **S1**, **S2** and **S3**, respectively. A high resistance to deformation and lower recovery ratio of the substrate **S1** as compared to **S2** and **S3** could indicate a reduced porosity and increased contact between the polymer chains of the substrate after compression [32]. This could negatively affect the release characteristics of the dosage form, for instance, when the folding of it for loading into hard gelatin capsule or forced adhesion of the solid foam to the buccal mucosa (if the oromucosal dosage form is in question) would be required. In addition, it appeared that the additives made the solid foam softer. This characteristic would be more desirable for oral dosage forms to minimize, among others, swallowing difficulties.

3.3. Characterization of the inkjet-printed dosage forms

3.3.1. Macroscopic and microscopic structure & solid state properties

Inkjet printing of the API-containing ink was successfully performed on all three selected substrates. The printed substrates stayed intact without any change in shape and overall appearance even after six months of storage in the ambient conditions, highlighting the suitability of the substrates for inkjet-printable pharmaceuticals.

The surface of all three substrates changed after inkjet printing of the API-containing ink due to a partial dissolution and/swelling of it by water-based ink during printing (Figs. 1 and 4). As a result, a non-porous smooth 'skin' layer was formed on the surface of the substrates after 20 and more printing passes. However, the formation of a continuous layer did not affect the ability of the substrate to hold a high amount of printed ink as at least 35 subsequent passes were successfully

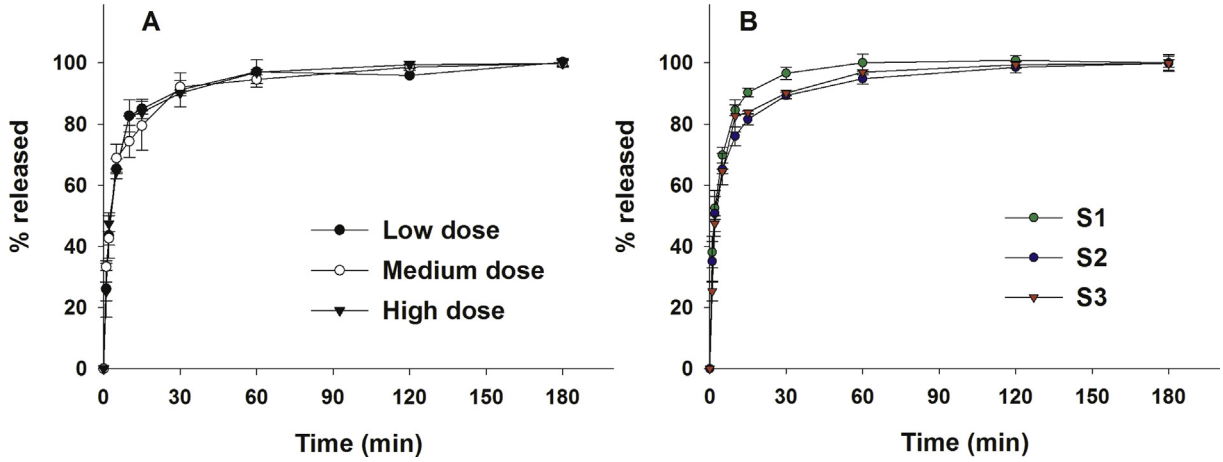

Fig. 6. The drug release profile printed on (A) the substrate **S3** at low, medium and high doses and (B) the substrates **S1**, **S2** and **S3** at high dose. Data are present as mean ± standard deviation, n = 3.

Table 6
Summary of the desired properties of the developed substrates: + + + very good; + + good and + deficient from the ideal substrate point of view.

Characteristics	Substrate, S1	Substrate, S2	Substrate, S3
Morphology	+ +	+ +	+ + +
Water penetration speed	+	+ + +	+ + +
Non-hygroscopicity	+ + +	+	+ +
Porosity	+	+ +	+ + +
Swelling index	+	+ +	+ + +
Flexibility	+	+ + +	+ +
Tensile strength	+ +	+	+ + +
Elongation at break	+	+ + +	+ +
Softness	+	+ +	+ + +
Recovery ratio	+	+ +	+ + +
Inkjet printing	+ + +	+ + +	+ + +
Immediate release	+ + +	+ + +	+ + +

printed on all three substrates. Overall, the formation of a 'skin' layer can be minimized by formulating the ink with a solvent that does not dissolve the substrate.

To assess the solid state properties of the inkjet-printed drug, DSC and MDSC measurements were performed. Thermal analysis of raw propranolol hydrochloride crystals revealed a sharp endothermic peak with onset at 161.7 °C, corresponding to the polymorphic form II [44]. However, it was not possible to detect any endothermic or exothermic events related to the melting, crystallization or glass transition of the printed drug, most probably due to a low drug content that was below the detection limit of the instrument and/or the presence of the drug molecularly dispersed in PG.

3.3.2. Drug content

The dosage forms were inkjet-printed as 1 cm^2 squares, containing seven different doses (Fig. 5). Manufacturing of flexible doses was achieved by printing different amount of subsequent layers (5–35 passes with 5 pass increment) of the API-containing ink on top of each other. Doses ranging from 0.52 to 4.68 mg per dosage form were prepared (Table 4). In average, 0.13 mg of the drug was printed per single pass with the only exception being the low dose on **S1,** where 0.10 mg was printed per pass. The reason for that is under current investigation. Despite that, the content uniformity was quite good as the standard deviation appeared to be very small (Table 5). The printing process was stopped after 35 passes due to the long printing time. However, it was still possible to incorporate a higher amount of the ink onto the porous substrate. Nevertheless, the inkjet-printed amount of the API per unit area of the developed solid foams was significantly higher in this study (4.6 mg/cm^2) as compared to the previous work, where commercially available edible rice paper and edible icing sheet or porous thin films were used as the substrates with maximum 0.85 mg/cm^2 [45] and 0.55 mg/cm^2 [21].

3.3.3. Release of the drug

The drug release from the printed dosage forms was determined for each substrate at low, medium and high printed doses, corresponding to 5, 25 and 35 passes, respectively. A very similar released profile was noticed for all printed dosage forms (Fig. 6). A fast release (over 55% of drug released) was detected in the first five minutes for all samples. A similar release kinetics of a inkjet-printed API onto electrospun fibers was noticed as well by Palo et al. [20]. Furthermore, all samples released at least 75% of the incorporated drug within the first 15 min. Dose-independent drug release profile from the printed dosage forms makes this manufacturing approach as a robust and a reproducible technique for production of flexible doses, i.e., personalized medicine.

Unlike the solid wafers, where the drug is embedded within the entire matrix of the dosage form and released slowly through the swollen gel layer of the different diffusion distance (depending on the thickness of the wafer) upon contact with the dissolution medium [37,46], the printed drug was predominantly deposited at and near the surface of the developed substrates. Therefore, the drug was immediately released from the surface of the substrate as diffusion through the swollen polymer was minimized.

3.4. Selection of the substrate for printable pharmaceuticals

Table 6 summarizes the properties of the developed substrates. It was obvious that none of the substrate possessed the optimal properties, regarding the studied characteristics. For instance, the most flexible substrate was at the same time the most hygroscopic. Therefore, either the substrate with a good balance between different properties should be selected or the substrate with the most desired properties should be chosen if those characteristics are critical for the manufacturing and application of a particular dosage form. For example, the porosity of the substrate would be an important characteristic for high-dose drugs. Thus, the carrier with the highest porosity should be preferred in order to incorporate the highest volume of the ink. In case of dosage forms for oromucosal administration, soft carriers should be selected. Patients with dysphagia would benefit the most from flexible dosage forms. It is also highly desired that all the dosage forms should have a high enough tensile strength and elongation at break to allow for general handling of the dosage forms without breaking.

4. Conclusions

Here we have described the fabrication of novel highly porous substrates intended for manufacturing of relatively high dose dosage forms using inkjet printing. Out of the studied preparation methods, only freeze-dried substrates possessed the desired characteristics, whereas HMPC-based carriers, containing hydrophilic additives, appeared to be the most suitable, regarding morphological, mechanical and absorption properties. Compared with the reported data from previous research studies, inkjet printing of higher doses of drug per unit area was successfully performed even though the ink composition was not optimal for the produced substrates. Extended studies should be focused on further optimization of the process parameters and formulation of the components in the substrates to achieve the most suitable carrier for drug-containing inks.

Acknowledgements

The authors would like to thank The Independent Research Fund Denmark, Technology and Production Sciences (FTP), grant number 12-126515/0602-02670B for financial support of this project. Prof. Niklas Sandler from Abo University Akademi is acknowledged for providing the opportunity to work with the advanced inkjet printer.

Appendix A. Supplementary material

Supplementary data to this article can be found online at https://doi.org/10.1016/j.ejpb.2019.01.004.

References

[1] FDA, Paving the way for personalized medicine, 2013.
[2] E. Cone, A. Gregory, Healthcare Gets Personal, Oxford, 2016. http://www.oxfordeconomics.com/my-oxford/projects/330885 (accessed 08.08.17).
[3] D.E. Pritchard, F. Moeckel, M.S. Villa, L.T. Housman, C.A. McCarty, H.L. McLeod, Strategies for integrating personalized medicine into healthcare practice, Per. Med. 14 (2017) 141–152, https://doi.org/10.2217/pme-2016-0064.
[4] N.J. Schork, Personalized medicine: time for one-person trials, Nature 520 (2015) 609–611, https://doi.org/10.1038/520609a.
[5] J. Lind, S. Kälvemark Sporrong, S. Kaae, J. Rantanen, N. Genina, Social aspects in additive manufacturing of pharmaceutical products, Expert Opin, Drug Deliv. 14 (2017), https://doi.org/10.1080/17425247.2017.1266336.
[6] M. Alomari, F.H. Mohamed, A.W. Basit, S. Gaisford, Personalised dosing: Printing a dose of one's own medicine, Int. J. Pharm. 494 (2015) 568–577, https://doi.org/10.1016/j.ijpharm.2014.12.006.
[7] R. Kolakovic, T. Viitala, P. Ihalainen, N. Genina, J. Peltonen, N. Sandler, Printing technologies in fabrication of drug delivery systems, Expert Opin. Drug Deliv. 10 (2013) 1711–1723, https://doi.org/10.1517/17425247.2013.859134.
[8] W.S. Cheow, T.Y. Kiew, K. Hadinoto, Combining inkjet printing and amorphous nanonization to prepare personalized dosage forms of poorly-soluble drugs, Eur. J. Pharm. Biopharm. 96 (2015) 314–321, https://doi.org/10.1016/j.ejpb.2015.08.012.
[9] M. Montenegro-Nicolini, V. Miranda, J.O. Morales, Inkjet printing of proteins: an experimental approach, AAPS J. 19 (2017) 234–243, https://doi.org/10.1208/s12248-016-9997-8.
[10] GlaxoSmithKline plc, Liquid dispensing technology (LDT), 2015. http://www.gsk.com/media/279688/liquid-dispensing-technology-leaflet.pdf (accessed 26.09.16).
[11] M. Edinger, D. Bar-Shalom, J. Rantanen, N. Genina, Visualization and non-destructive quantification of inkjet-printed pharmaceuticals on different substrates using Raman spectroscopy and Raman chemical imaging, Pharm. Res. 34 (2017) 1023–1036, https://doi.org/10.1007/s11095-017-2126-2.
[12] N. Genina, E.M. Janßen, A. Breitenbach, J. Breitkreutz, N. Sandler, Evaluation of different substrates for inkjet printing of rasagiline mesylate, Eur. J. Pharm. Biopharm. 85 (2013) 1075–1083.
[13] A.B.M. Buanz, M.H. Saunders, A.W. Basit, S. Gaisford, Preparation of personalized-dose salbutamol sulphate oral films with thermal ink-jet printing, Pharm. Res. 28 (2011) 2386–2392, https://doi.org/10.1007/s11095-011-0450-5.
[14] D. Raijada, N. Genina, D. Fors, E. Wisaeus, J. Peltonen, J. Rantanen, N. Sandler, A step towards development of printable dosage forms for poorly soluble drugs, 102 (2013) 3694–3704. doi: 10.1002/jps.23678.
[15] L. Hirshfield, A. Giridhar, L.S. Taylor, M.T. Harris, G.V. Reklaitis, Dropwise additive manufacturing of pharmaceutical products for solvent-based dosage forms, J. Pharm. Sci. 103 (2014) 496–506, https://doi.org/10.1002/jps.23803.
[16] N. Genina, D. Fors, M. Palo, J. Peltonen, N. Sandler, Behavior of printable formulations of loperamide and caffeine on different substrates - effect of print density in inkjet printing, Int. J. Pharm. 453 (2013) 488–497.
[17] R.P. Dixit, S.P. Puthli, Oral strip technology: overview and future potential, J. Control. Release 139 (2009) 94–107, https://doi.org/10.1016/j.jconrel.2009.06.014.
[18] J. Pardeike, D.M. Strohmeier, N. Schrödl, C. Voura, M. Gruber, J.G. Khinast, A. Zimmer, Nanosuspensions as advanced printing ink for accurate dosing of poorly soluble drugs in personalized medicines, Int. J. Pharm. 420 (2011) 93–100, https://doi.org/10.1016/j.ijpharm.2011.08.033.
[19] E. Elele, Y. Shen, B. Khusid, E. Elele, Y. Shen, B. Khusid, Electrodeless electrohydrodynamic printing of personalized medicines, Appl. Phys. Lett. 97 (2010), https://doi.org/10.1063/1.3524512.
[20] M. Palo, K. Kogermann, I. Laidmäe, A. Meos, M. Preis, J. Heinämäki, N. Sandler, Development of oromucosal dosage forms by combining electrospinning and inkjet printing, Mol. Pharm. 14 (2017) 808–820, https://doi.org/10.1021/acs.molpharmaceut.6b01054.
[21] E. Elele, Y. Shen, R. Susarla, B. Khusid, G. Keyvan, B. Michniak-Kohn, Electrodeless elctrohydrodynamic drop-on-demand encapsulation of drugs into porous polymer films for fabrication of personalized dosage units, J. Pharm. Sci. 101 (2012) 2523–2533, https://doi.org/10.1002/jps.
[22] K. Siimon, H. Siimon, M. Järvekülg, Mechanical characterization of electrospun gelatin scaffolds cross-linked by glucose, J. Mater. Sci. - Mater. Med. 26 (2015) 37, https://doi.org/10.1007/s10856-014-5375-1.
[23] M. Zhang, X. Zhao, G. Zhang, G. Wei, Z. Su, E. Zussman, D.J. Gengzang, X.L. Xu, S.H. Yan, M.B. Linder, J. Ahopelto, Electrospinning design of functional nanostructures for biosensor applications, J. Mater. Chem. B 5 (2017) 1699–1711, https://doi.org/10.1039/C6TB03121H.
[24] X. Liu, S.G. Baldursdottir, J. Aho, H. Qu, L.P. Christensen, J. Rantanen, M. Yang, Electrospinnability of Poly Lactic-co-glycolic Acid (PLGA): the role of solvent type and solvent composition, Pharm. Res. 34 (2017) 738–749, https://doi.org/10.1007/s11095-017-2100-z.
[25] L. Rey, J.C. May, D.Q. Wang, Freeze-drying/lyophilization of pharmaceutical and biological products, in: L. Rey, J.C. May (Eds.), Free. Pharm. Biol. Prod., 3rd ed., Informa Healthcare, New York, London, 2010, pp. 1–564. http://www.gbv.de/dms/bs/toc/376091975.pdf (accessed 08.08.17).
[26] M.H. Dehghan, M. Girase, Freeze-dried Xanthan/Guar Gum Nasal Inserts for the Delivery of Metoclopramide Hydrochloride, Iran. J. Pharm. Res. IJPR. 11 (2012) 513–521 (accessed August 11, 2017), http://www.ncbi.nlm.nih.gov/pubmed/24250474.
[27] M. Khorasani, J.M. Amigo, J. Sonnergaard, P. Olsen, P. Bertelsen, J. Rantanen, Visualization and prediction of porosity in roller compacted ribbons with near-infrared chemical imaging (NIR-CI), J. Pharm. Biomed. Anal. 109 (2015) 11–17, https://doi.org/10.1016/j.jpba.2015.02.008.
[28] N. Genina, D. Fors, H. Vakili, P. Ihalainen, L. Pohjala, H. Ehlers, I. Kassamakov, E. Haeggström, P. Vuorela, J. Peltonen, N. Sandler, Tailoring controlled-release oral dosage forms by combining inkjet and flexographic printing techniques, Eur. J. Pharm. Sci. 47 (2012) 615–623, https://doi.org/10.1016/j.ejps.2012.07.020.
[29] P. Modamio, C.F. Lastra, O. Montejo, E.L. Marifio, Development and validation of liquid chromatography methods for the quantitation of propranolol, metoprolol, atenolol and bisoprolol: Application in solution stability studies, Int. J. Pharm. 130 (1996) 137–140, https://doi.org/10.1016/0378-5173(95)04257-1.
[30] A.F. Borges, C. Silva, J.F.J. Coelho, S. Simões, Oral films: Current status and future perspectives, J. Control. Release 206 (2015) 1–19, https://doi.org/10.1016/j.jconrel.2015.03.006.
[31] A. Krekeler, Formulation development and manufacturing of oral film preparations, in: PBP Worldmeeting, Glasgow, the United Kingdom, 2016.
[32] J.S. Boateng, A.D. Auffret, K.H. Matthews, M.J. Humphrey, H.N.E. Stevens, G.M. Eccleston, Characterisation of freeze-dried wafers and solvent evaporated films as potential drug delivery systems to mucosal surfaces, Int. J. Pharm. 389 (2010) 24–31, https://doi.org/10.1016/j.ijpharm.2010.01.008.
[33] M.A.A. Kassem, A.N. ElMeshad, A.R. Fares, Lyophilized sustained release mucoadhesive chitosan sponges for buccal buspirone hydrochloride delivery: formulation and in vitro evaluation, AAPS PharmSciTech. 16 (2015) 537–547, https://doi.org/10.1208/s12249-014-0243-3.
[34] A. Nussinovitch, R. Velez-Silvestre, M. Peleg, Compressive characteristics of freeze-dried agar and alginate gel sponges, Biotechnol. Prog. 9 (1993) 101–104, https://doi.org/10.1021/bp00019a015.
[35] V. Garsuch, J. Breitkreutz, Novel analytical methods for the characterization of oral wafers, Eur. J. Pharm. Biopharm. 73 (2009) 195–201, https://doi.org/10.1016/j.ejpb.2009.05.010.
[36] I. Ayensu, J.C. Mitchell, J.S. Boateng, In vitro characterisation of chitosan based xerogels for potential buccal delivery of proteins, Carbohydr. Polym. 89 (2012) 935–941, https://doi.org/10.1016/j.carbpol.2012.04.039.
[37] J.S. Boateng, K.H. Matthews, A.D. Auffret, M.J. Humphrey, H.N. Stevens, G.M. Eccleston, In vitro drug release studies of polymeric freeze-dried wafers and solvent-cast films using paracetamol as a model soluble drug, Int. J. Pharm. 378 (2009) 66–72, https://doi.org/10.1016/j.ijpharm.2009.05.038.
[38] J.S. Vrentas, C.M. Vrentas, Surface concentration effects in the drying of solvent-coated polymer films, J. Appl. Polym. Sci. 60 (1996) 1049–1055, https://doi.org/10.1002/(SICI)1097-4628(19960516)60:7<1049::AID-APP16>3.0.CO;2-W.
[39] I. Ayensu, J.C. Mitchell, J.S. Boateng, Development and physico-mechanical characterisation of lyophilised chitosan wafers as potential protein drug delivery systems via the buccal mucosa, Colloids Surfaces B Biointerfaces. 91 (2012) 258–265, https://doi.org/10.1016/j.colsurfb.2011.11.004.
[40] F. Kianfar, I. Ayensu, J.S. Boateng, Development and physico-mechanical characterization of carrageenan and poloxamer-based lyophilized matrix as a potential buccal drug delivery system, Drug Dev. Ind. Pharm. 40 (2014) 361–369, https://doi.org/10.3109/03639045.2012.762655.

[41] T. Rogers, Hypromellose, in: C. Rowe, P. Sheskey, M. Quinn (Eds.), Handb. Pharm. Excipients, 6th ed., Pharmaceutical Press and American Pharmacists Association, London Chicago, 2009, pp. 326–329.
[42] J. Collett, Poloxamer, in: C. Rowe, P. Sheskey, M.E. Quinn (Eds.), Handb. Pharm. Excipients, 6th ed., Pharmaceutical Press and American Pharmacists Association, 2009, pp. 506–509.
[43] H. Lim, S.W. Hoag, Plasticizer effects on physical-mechanical properties of solvent cast soluplus® films, AAPS PharmSciTech. 14 (2013) 903–910, https://doi.org/10.1208/s12249-013-9971-z.
[44] M. Bartolomei, P. Bertocchi, M. Cotta Ramusino, E. Ciranni Signoretti, Thermal studies on the polymorphic modifications of (R, S) propranolol hydrochloride, Thermochim. Acta. 321 (1998) 43–52, https://doi.org/10.1016/S0040-6031(98)00438-9.
[45] H. Vakili, J.O. Nyman, N. Genina, M. Preis, N. Sandler, Application of a colorimetric technique in quality control for printed pediatric orodispersible drug delivery systems containing propranolol hydrochloride, Int. J. Pharm. 511 (2016) 606–618, https://doi.org/10.1016/j.ijpharm.2016.07.032.
[46] R. Shaikh, T.R. Raj Singh, M.J. Garland, A.D. Woolfson, R.F. Donnelly, Mucoadhesive drug delivery systems, J. Pharm. Bioallied Sci. 3 (2011) 89–100, https://doi.org/10.4103/0975-7406.76478.